Towards optimization of 5G NR transport over fiber links performance in 5G Multi-band Networks: An OMSA model approach

Optical Fiber Technology xxx (xxxx) xxx

Contents lists available at ScienceDirect

Optical Fiber Technology

journal homepage: www.elsevier.com/locate/yofte

Regular Articles

Towards optimization of 5G NR transport over fiber links performance in 5G Multi-band Networks: An OMSA model approach

Muhammad Usman Hadi [1]

School of Engineering, Ulster University, BT15 1AP Belfast, United Kingdom

ARTICLE INFO

Keywords:
Digital predistortion
Radio over fiber
Optimized magnitude selective affine
Error vector magnitude
Impairment mitigation

ABSTRACT

The application of analog radio over fiber (A-RoF) systems for 5G new radio (NR) multiband waveforms presents challenges, including nonlinearity introduced by the Mach Zehnder Modulator and the dispersion and attenuation of the optical signal over long fiber lengths. To address these challenges, this paper proposes a new version of the magnitude-selective affine (MSA) model, named the optimized magnitude-selective affine (OMSA) model, which incorporates a power-reliant weighting function to improve performance while reducing complexity via Digital Predistortion (DPD). The OMSA model is tested using 5G NR signals at 10 GHz with 50 MHz and flexible-waveform signals at 2.14 GHz with a 20 MHz bandwidth, transmitted over a 10 km fiber length using a Mach Zehnder Modulator and a 1550 nm optical carrier. The performance of the OMSA model is compared to the MSA and generalized memory polynomial (GMP) models in terms of adjacent channel power ratio, error vector magnitude, and complexity. The results show that the OMSA model outperforms the MSA and GMP models in terms of performance reducing the error vector magnitude to 1.9% as compared to 4% and 3% in case of GMP and MSA respectively. Additionally, in terms of complexity measured via coefficients, OMSA is 168 times more efficient as compared to GMP and offers 1.93 times higher efficiency as compared to MSA while maintaining lower complexity. The experimental demonstration of 5G NR multiband waveforms over A-RoF links using the OMSA model represents a significant step towards the practical implementation of high-performance, low-complexity 5G NR systems over fiber-optic links and provides a promising solution to the challenges associated with DPD linearization for A-RoF systems.

1. Introduction

The use of radio over fiber (RoF) technology is becoming increasingly popular for 5G and 6G systems due to its capability to provide fast and high-capacity wireless communication [1]. RoF utilizes optical fibers to transmit radio signals, resulting in increased bandwidth and longer transmission distances in comparison to traditional wireless systems. This feature of RoF technology helps to address the increasing need for data transfer in 5G and 6G networks [2].

Furthermore, RoF systems offer improved isolation between different wireless users, leading to better overall performance and dependability of the network. Additionally, RoF systems can be seamlessly integrated with existing optical fiber infrastructure, which helps to minimize the cost and complexity of implementing 5G and 6G networks [3,4].

RoF systems can also support a variety of wireless technologies, such as millimeter wave, terahertz, and other cutting-edge technologies that are expected to be a vital component of 5G and 6G networks. By utilizing the capabilities of RoF, 5G and 6G networks can offer enhanced coverage, faster data rates and reduced latency for a wide range of applications. Fig. 1 illustrates the Radio over fiber (RoF) based Optical fronthaul (OFH) system.

Radio over Fiber (RoF) links can be affected by nonlinear issues caused by the components of the link, which can be mitigated through linearization techniques. RoF has different forms, including analogue RoF (A-RoF), digital RoF, and sigma–delta RoF (δRoF) linkages. While A-RoF can experience signal degradation over long distances, digital RoF is more cost-effective for longer connections but comes with the added expense of higher bandwidth resolution and additional signal processing. Additionally, fronthaul networks can have low efficiency and increased data traffic demand. RoF can overcome the CPRI bottleneck using a 1-bit ADC, but this creates a lot of quantization noise, making the technique more challenging and requiring the use of a passband filter on the receiver side. Despite this, A-RoF is still preferred over digital and

E-mail address: m.hadi@ulster.ac.uk.
[1] Orcid: https://orcid.org/0000-0002-3363-2886.

https://doi.org/10.1016/j.yofte.2023.103358
Received 27 January 2023; Received in revised form 10 April 2023; Accepted 5 May 2023

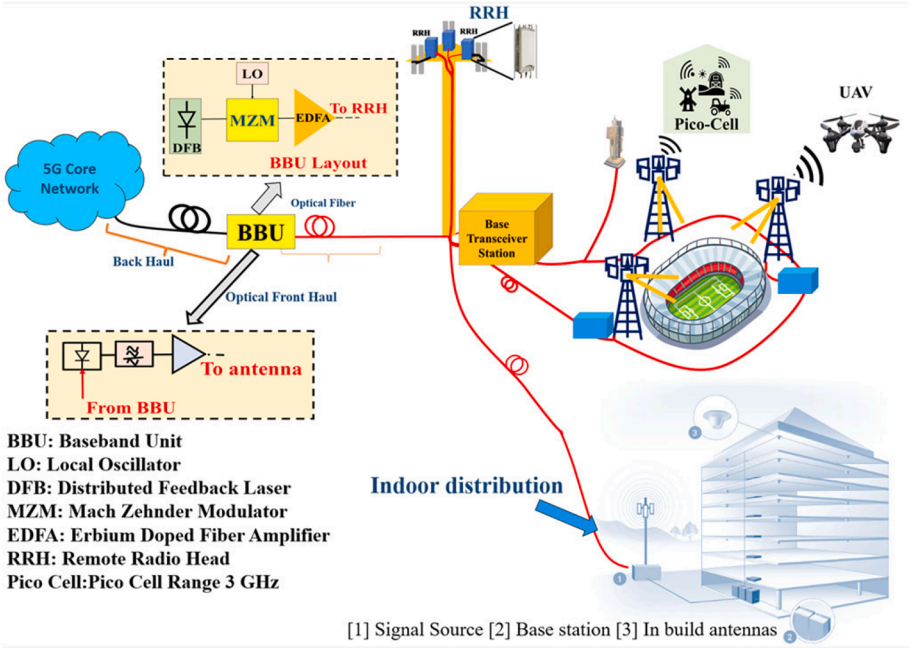

Fig. 1. A system is presented where the baseband unit (BBU) is connected to the optical front haul (OFH) for backhaul and the signal is then transmitted from the transceiver station.

sigma-delta RoF due to its simplicity, affordability, and well-established structure [5,6].

One of the main challenges in RoF systems is the presence of various impairments that can negatively impact the quality of the transmitted signal. These impairments include nonlinear effects of laser, optical fiber dispersion, and noise, which can significantly limit the system's performance. Digital pre-distortion (DPD) is a powerful technique for counteracting these impairments to improve the performance of the system. DPD addresses the impairments in the RoF link, resulting in an overall improvement in the performance of RoF systems. DPD treats all these impairments in RoF system as a black box and finds the inverse nonlinear response to that black box. When cascaded together, the overall response is linear which removes all these impairments [7,8].

The limitations imposed by microwave and optical components restrict the use of Analog Radio over Fiber (A-RoF). Many linearization techniques have been proposed to overcome these limitations, but they have been criticized for their insufficient bandwidth, high complexity, and the need for feedback links, which is a time-consuming process. In recent years, Digital Predistortion (DPD) solutions have become more complex as the implementation requirements of cellular network communications have increased. This is further compounded by the use of more complex power amplifier designs, such as MIMO and beamforming, which are used to improve system performance at these frequencies. The goal of DPD is to create a compact model that compensates for the nonlinearity of the RoF, resulting in a highly linear output signal with the fewest coefficients possible. However, when training DPD coefficients, overfitting and ill-conditioning can be an issue. Therefore, the reduction of DPD dimensionality, overfitting, and extraction have become important areas of research.

Several different DPD architectures can be applied to RoF systems, each with their own advantages and disadvantages. One of these techniques is the Generalized Memory Polynomial (GMP) architecture, which is a model-based approach that uses a polynomial model to represent the nonlinear behaviour of the RoF system [4,9]. However, it requires accurate modelling of the system, which can be challenging. Another technique is the Memory Polynomial (MP) architecture, which is a simplified version of the GMP architecture [9–10], but less flexible. Canonical Piecewise Linearization (CPWL) architecture is another method that can be used to approximate the nonlinear transfer function of a radio frequency (RF) for RoF systems [10]. This architecture has good performance, but the complexity is high.

The Magnitude Selective Affine (MSA) method is another proposed architecture that provides good performance, but the complexity is still high. To reduce the complexity of the MSA architecture, one way is to combine the different stages into a single stage, using a more flexible and powerful DPD technique such as the GMP approach.

The desire for further linearization to achieve better results has led to an increased focus on using machine learning (ML) techniques [11–13]. In previous studies, analog RoF was used for successful integration trials in fiber wireless systems, but no linearization was used and the system was limited to 64 quadrature amplitude modulation (QAM). Other studies have achieved 25 Gbauds with 64 QAM, but linearization methods were not used to improve performance. Dual-wavelength linearization has been used to suppress second and third-order nonlinearities, but it is dependent on the wavelength. Digital Post Distortion (DPD) has also been proposed to compress all order nonlinear distortion components, but it requires a high-speed digitizer. Recently, machine learning (ML) techniques have been proposed to address nonlinearities caused by factors such as fiber nonlinearity, modulation impairments, laser chirp, and laser nonlinearities in digital predistortion (DPD) using neural network. Additionally, analog DPD has been used to linearize the complete radio over fiber (RoF) system and suppress third-order intermodulation distortion (IMD3) for phase maintenance, but it does not address second-order IMDs. Direct DPD has also been proposed to linearize the combined effects of fiber chromatic dispersion and laser chirp for long fiber lengths. While conventional DPD methods can alleviate impairments in the laser and overall RoF link, they require a large amount of training data and high complexity.

Recently, a new DPD technique that combines Volterra series with deep neural networks was proposed to improve the linearization performance of RoF systems [14]. The proposed DPD technique can accurately capture the nonlinearity of high-power amplifiers and improve the overall system performance. The proposed DPD technique requires a large amount of training data and may have higher computational complexity compared to traditional DPD techniques. Similarly, Xiaoran Xie et al. proposed a hybrid DPD technique that combines the analog and

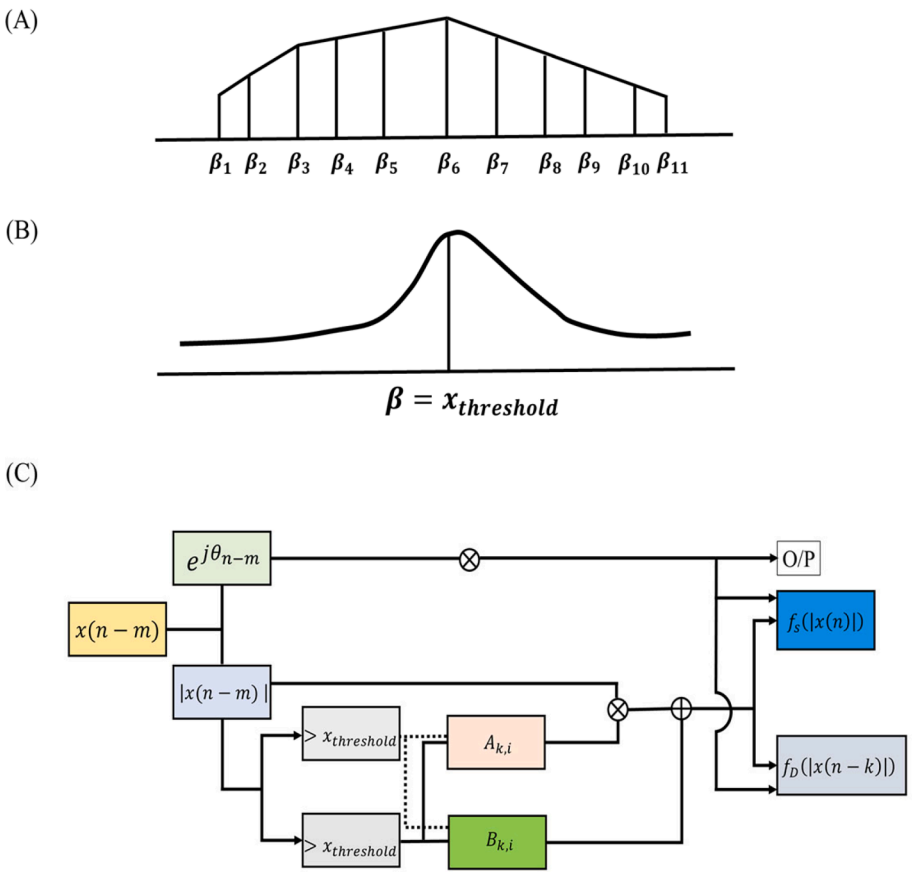

Fig. 2. shows the illustration of: (A) Magnitude selective affine (MSA) architecture. (B) Optimized magnitude selective affine (OMSA). (C) Proposed OMSA model structure state diagram.

digital pre-distortion methods to improve the efficiency and accuracy of RoF systems [15]. Recently, Jacopo Nanni et al. suggested short-λ-VCSELs DPD over pre-existent G-652 Infrastructures Radio over Fiber systems for a 2Km transmission distance [16]. The proposed technique can reduce the number of digital-to-analog and analog-to-digital conversions required, thus improving the system's overall efficiency. The proposed technique requires additional analog components, which can increase the overall cost and complexity of the system. Similarly, adaptive DPD algorithm for RoF links that utilizes the least-mean-square (LMS) algorithm to dynamically adjust the DPD coefficients based on the input signal power level was discussed in a recent survey paper [17]. The discussed schemes can reduce the computational complexity and improve the accuracy of DPD systems [17]. The proposed algorithm may require additional hardware to implement, which can increase the overall cost and complexity of the system.

In this paper, we propose a 5G NR- multiband for Radio over Fiber link outfitted with an optimized magnitude selective affine (OMSA) method to cover enhanced mobile broadband (eMBB) situations for 2.14 GHz and 10 GHz, correspondingly. We show experimentally that OMSA further reduces the complexity with better or at least similar performance to that of MSA by using a weighted function as a nonlinear operator to accurately capture the nonlinear behaviour of the system being modelled, which can lead to a reduction in the number of segments and improvement in the accuracy of the model. This means that it will also lead to a reduction in the number of coefficients needed. This helps to make the model more efficient and simpler to use. The experimental results demonstrate that the OMSA model has lower complexity than the MSA model while achieving a slightly better performance that is assessed in terms of computations, error vector magnitude (EVM) or adjacent channel power ratio (ACPR). The main contributions of the paper are summarized below:

1. To experimentally demonstrate a 5G NR-multiband for 10 km Radio over Fiber link for eMBB situations at 2.14 GHz and 10 GHz.
2. An OMSA method is proposed that uses a weighted function as a nonlinear operator to capture the system's nonlinear behaviour and reduce the number of segments and coefficients needed.
3. The article comprises DPD methodology based on OMSA with all of its mathematical frameworks, and the selection of parameters to reduce the complexity and enhance the performance.
4. The performance is compared with baseline Volterra methods such as GMP [9–11]. In addition to GMP method, the comparison consists of authors earlier proposed CPWL based on MSA methods [14].
5. Showed that OMSA model has better performance in terms of error vector magnitude (EVM), or adjacent channel power ratio (ACPR) as compared to baseline GMP and earlier proposed MSA methods. The complexity analysis is reported in terms of the number of coefficients, time, memory and data consumption.

The proposed OMSA architecture and theory in Section 2 is discussed followed by comparative architecture summarized in Section 3. The experimental setup in Section 4 is discussed followed by the presentation of the experimental results in Section 5. The conclusions are provided in Section 6.

2. Dpd integration based on optimized msa

The essential modelling for DPD is considered here. The effective form of MSA function that was proposed earlier can be expressed as [18]:

$$\sum_{m=0}^{M}\sum_{k=0}^{K}\sum_{l=1}^{L} c_{m,k,l}^{(1)} \left|x(n-k)\right|^2 - \beta_l \left|x(n-m-k)\right.$$

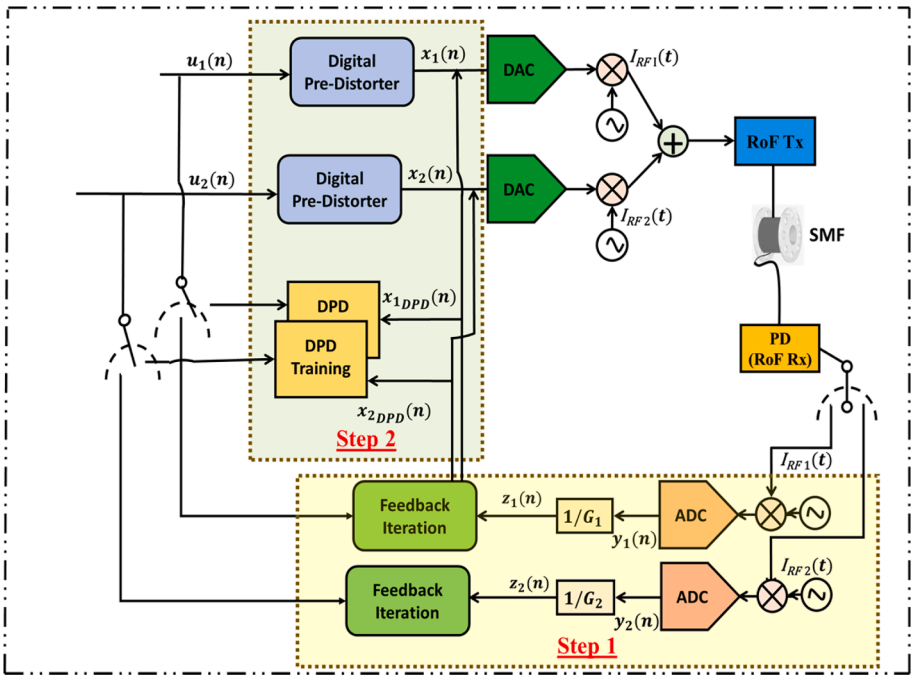

Fig. 3. A link training scheme for RoF that is compatible with various architectures, including GMP, MSA and OMSA.

$$= \sum_{m=0}^{M}\sum_{k=0}^{K} x(n-m-k)\left(\sum_{l=1}^{L} c_{m,k,l}^{(1)} \left| |x(n-k)|^2 - \beta_l \right|\right)$$

$$= \sum_{m=0}^{M}\sum_{k=0}^{K} u_{m,k}^{(1)}(n-k)x(n-m-k) \tag{1}$$

$$u_{m,k}^{(1)}(n-k) = \sum_{l=1}^{L} c_{m,k,l}^{(1)} \left| |x(n-k)|^2 - \beta_l \right|$$

$$= \begin{cases} A_{m,k,1}^{(1)} |x(n-k)|^2 + B_{m,k,1}^{(1)}, 0 \le |x(n-k)|^2 < \beta_1 \\ \vdots \\ A_{m,k,L}^{(1)} |x(n-k)|^2 + B_{m,k,L}^{(1)}, \beta_{L-1} \le |x(n-k)|^2 < \beta_L \end{cases} \tag{2}$$

In Eq. (1), the linear model coefficients for each zone of the MSF function $u_{m,k}^{(1)}()$ are represented by $A_{m,k,l}^{(1)}$ and $B_{m,k,l}^{(1)}$. In Eq. (2), the input baseband signal is represented by $x(n)$, and the output baseband signal is characterised by $y(n)$. The dimension of the FIR filter is characterized by K, and the memory depth is symbolized by M. The number of partitions is represented by L, and the threshold is represented by β_l. The model coefficients are embodied by $c_{m,k,l}^{(1)}, c_{m,k,l}^{(2)}, c_{m,k,l}^{(3)}, c_{m,k,l}^{(4)}$.

In equation (1), the input power terms are evaluated against specific thresholds for determining the offset and linear gain for the MSA function, eliminating the need for a square root calculation. The overall model represented by equation (1) can be represented using the MSA function as follows:

$$y(n) = \sum_{m=0}^{M} c_m x(n-m)$$

$$+ \sum_{m=0}^{M} \left(A_{k,1}^{(m)} |x(n-m)|^2 + B_{k,1}^{(m)}\right) e^{j\theta(n-m)}$$

$$+ \sum_{m=0}^{M} \left(A_{k,21}^{(m)} |x(n-m)|^2 + B_{k,21}^{(m)}\right) e^{j\theta(n-m)} |x(n)|$$

$$+ \cdots \beta_{k-1} \le |x(n)| \le \beta_k \tag{3}$$

In equation (3), $A_{m,k,l}^{(i)}$ and $B_{m,k,l}^{(i)}$ are the coefficients defined for each zone of the MSF linear model function $u_{m,k}^{(i)}()$. These coefficients are estimated using a least squares (LS) algorithm.

The precision of the MSA paradigm can be enhanced by reducing the number of segments, as indicated in Fig. 2(a). In the MSA model, the input waveform is partitioned into several zones based on the β values. Each state has its model parameters, and all the segments can be considered a collection of affine functions. In contrast, the OMSA model divides the input signal using β as a specific threshold and replaces the affine functions with subjective functions that depend on the input power. The subjective functions in the OMSA model can be expressed as:

$$\prod_s (x(n)) = \frac{1}{2}\left[1 + tanh\left(S(|x(n)|) * \left(\frac{(1-k)}{k} * k\right)\right)\right] \tag{4}$$

$$\prod_D (x(n)) = \frac{1}{2}\left[1 + tanh\left(S(|x(n)|) * \left(\frac{1}{k^2}.i\right)\right)\right] \tag{5}$$

Here

$$S(x(n)) = \left(1 - \frac{|x(n)|}{x_{threshold}.|x|_{max}}\right) \tag{6}$$

In the OMSA model, the subjective functions $\prod_s()$ and $\prod_D()$ are functions that map the absolute value of the input signal to the corresponding weighting function for the dynamic and static terms, correspondingly. The input signal is divided into k segments using a threshold value β. In this paper, k is set to the value of 2. The || operator performs the absolute value operation on the input signal. The use of these weighting functions can improve the model precision by reducing the number of segments and taking into account the power of the input signal. With the updates explained in Eq. (5)-(6), the OMSA with the updates will become:

$$y(n)_{OMSA} = \sum_{m=0}^{M} c_m x(n-m)$$

$$+ f_s(x(n)) * \left(A_{k,i}|x(n)| + B_{k,i}\right) e^{j\theta(n)}$$

$$+ \sum_{m=1}^{M} f_D(x(n-m)) * \left(A_{k,i}|x(n-m)| + B_{k,i}\right) e^{j\theta(n-m)}$$

$$+ f_s(x(n)) * \left(A_{k,i}|x(n)| + B_{k,i}\right) e^{j\theta(n)} |x(n)|$$

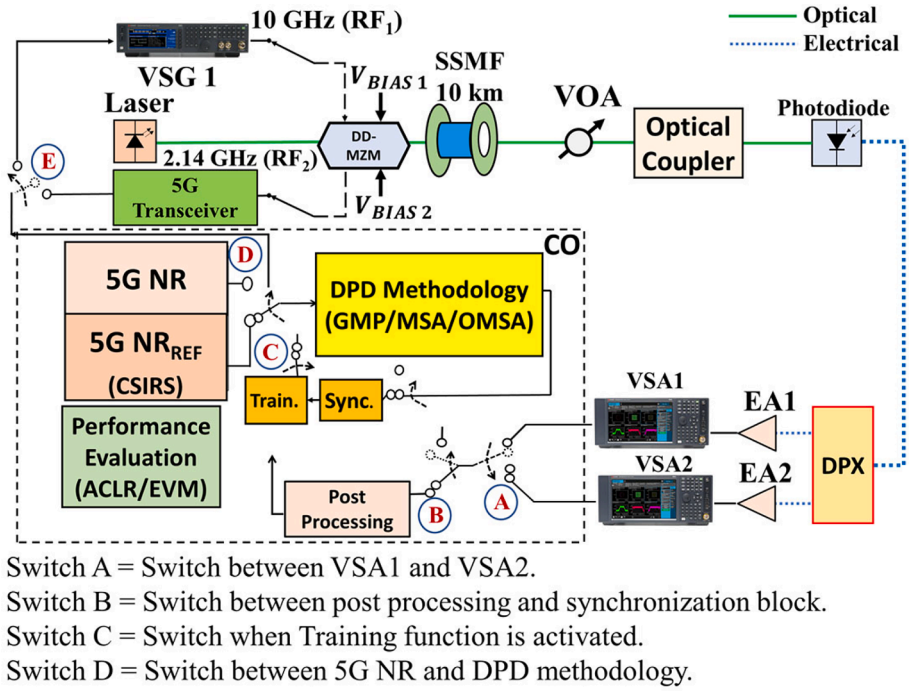

Fig. 4. Block diagram of the experimental block schematic for the linearization study.

$$+\sum_{m=1}^{M} f_D(x(n-m))*\left(A_{k,i}|x(n-m)|+B_{k,i}\right)e^{j\theta(n-m)}|x(n)| \tag{7}$$

$x(n)$ and $y(n)$ shows the corresponding input and output at the baseband. The OMSA model uses a weighted function that is more flexible and power-dependent, allowing for a reduction in the number of amplitude segments compared to the MSA model. The proposed OMSA structure is shown in Fig. 2(C).

The DPD coefficients are computed during the training period by determining the DPD model coefficients, as depicted in Fig. 3. $z(n)$ is the predistorter's input, which comes through the RoF $y(n)$ here, $z(n) = \frac{y(n)}{G}$, and G is the gain link. This approach consists of two basic phases. The first stage is to set up a negative feedback loop to acquire an input signal that can be classified as a DPD waveform signal, and then the second step is to calculate the DPD model parameters.

3. State of the art baseline architectures

DPD linearization has been employed using different methodologies. One of the most significant and widely employed method is using Volterra series method such as generalized memory polynomials also called as GMP. The GMP method has been shown to be successful for linearizing Power Amplifiers. The use of Digital predistortion for linearizing the RoF link has been demonstrated in previous studies [7,9–11]. The GMP approach, unlike the MP method, considers both the diagonal and cross components, which is why it outperforms MP. In the following sections, the comparison will be made with GMP only from the Volterra series as it has been shown to provide improved performance compared to MP [9].

The baseline conventional GMP architecture is expressed as:

$$y(n) = \sum_{k=0}^{k_a-1}\sum_{q=0}^{Q_a-1} x(n-q)c_{kq}|x(n-q)|^k$$

$$+\sum_{k=1}^{k_b}\sum_{q=0}^{Q_b-1}\sum_{r=1}^{R_b} x(n-q)d_{kqr}|x(n-q-r)|^k$$

$$+\sum_{k=1}^{k_c}\sum_{q=0}^{Q_c-1}\sum_{r=1}^{R_c} |x(n-q+r)|^k e_{kqr}x(n-q)$$

where $x(n)$ and $y(n)$ are the DPD input and output respectively. The c_{kq}, d_{kqr} and e_{kqr} signify the signal-envelope; signal-lagging envelope and signal-leading envelope complex coefficients, correspondingly. K_a, K_b, K_c represent maximum nonlinearity coefficients, Q_a, Q_b, Q_c shows memory depths.q, r and k are the symbols of the memory and nonlinearity index while R_c demonstrates the leading delay tap lengths and R_b presents the lagging delay tap lengths.

4. Experimental testbed

The experimental setup schematic, as shown in Fig. 4, includes a Mach Zehnder modulator (MZM) from iXblue dual drive, a 1550 nm laser, a 10 km standard single mode fiber (SSMF) and a R402 PIN photodetector to convert the received wave back to the electrical domain. The signals are separated by a diplexer and then sent to distinct vector signal analysers. The 5G transceiver provides RF2, a 2.14 GHz flexible waveform signal, while the Keysight N5172B Vector Signal Generator VSG1 sends a 10 GHz RF1 5G NR waveform. The DPD technique includes three steps. It uses a 5G NR with 2.14 GHz (20 MHz) and 10 GHz (50 MHz) to check the efficacy of the proposed OMSA method and compare it to previously validated DPD methods such as MSA and GMP [8–11,13–14].

For this, a multiband 5G NR setup for eMBB environments operating at 2.14 GHz and 10 GHz is used, with a DPD block added for enhancing the performance via linearization. The phase and amplitude responses are ensured to be opposite to those produced from electrical amplifiers EA1 and EA2 by using the DPD operation for training until the error converges.

Time synchronization is performed using a 20 MHz/106 resource blocks Channel State Information Reference Signal (CSI-RS). The received and input reference signals are correlated, and the power delay profile (PDP) is assessed to determine the first path of arrival as suggested by 3GPP [19.20].

In the end, the pre-distorted baseband waveforms are sent to the DPD

Table 1
Optical Link Parameters.

Parameters	Values
Waveforms	$f_{c1} = 2.14 \times 10^9$ Hz $f_{c2} = 10 \times 10^9$ Hz F/ G/ O- FDM signal Modulation Data Rate = 256 QAM
Modulator Laser	Wavelengthλ = 1550 nm DD-MZM
Fiber	Single Mode Fiber Link length = 10 km Fiber Dispersion = 17 $\frac{\text{ps}}{\text{nmkm}}$ Attenuation = 0.33 $\frac{\text{dB}}{\text{km}}$
Photoreceiver	$\mathscr{R}$, *Responsivity* = 0.69 A/W

block, where they are upconverted to their f_c by VSGs before being transmitted over the optical connection. The signal received by the photodiode is passed through a diplexer DPX that separates multiband signals before being sent to the DPD block for the training phase. For the DPD validation stage, the switches are flipped in the opposite direction. The DPD validation phase uses real-time 5G NR frames to confirm the effectiveness of the DPD process. Since RoF impairments tend to change gradually due to component ageing and thermal effects, there is no need for real-time adaptation of DPD coefficients. Table 1 provides a summary of the various component values used in this study.

5. Experimental outcomes and discussion

The proposed OMSA-DPD technique and MSA are used with specific parameters ($K = L = 4$, $M = 3$) and compared to the GMP method (K = Q = 3) as described in a previous study [10]. The effectiveness of the OMSA-DPD technique is experimentally evaluated through spectral regrowth, EVM, and ACPR, as described in [18]. The OMSA-DPD method aims to simplify the process and improve performance when compared to previous methods such as MSA, CPWL, GMP, and no DPD methods. Fig. 5 shows the electrical spectra at the PD output at 2.14 and 10 GHz, respectively, and demonstrates the effectiveness of the OMSA-DPD method in recovering 25 dBm peak to peak and reducing ACPR by 18 dB, compared to 10 dB for MSA and 6 dB for GMP.

In Fig. 6(a), the EVM is displayed for varying RF input power with and without DPD. It can be seen that the OMSA-based DPD method outperforms the other methods. In addition, OMSA achieves 3% EVM while MSA achieves 3.5% as compared to 11.2 % EVM without DPD. This is evident that OMSA with optimization has achieved a similar performance as compared to MSA. The Adjacent Channel Leakage Ratio (ACLR) is evaluated in Fig. 6(b) which measures the interference outside the useful bandwidth. Method. OMSA achieves −47.4 dBc while MSA achieves −45 dBc as compared to −28 dBc as compared to non-compensated cases, which is below the −45 dBc set by 3GPP [19,20].

The EVM obtained with OMSA architecture are in line with the 3.5% EVM limit set by the release 3GPP TR 21.916 V16.2.0 (2022–06) [21] and latest release 17 3GPP TS 36.141 version 17.5.0 Release 17 [22]. Although the results presented indicate that the OMSA method has better performance than the MSA method, the main advantage of OMSA is its lower complexity. The OMSA-DPD method is more efficient than the MSA method as it requires fewer multiplications and has less complexity, as seen in Table 2.

Specifically, the OMSA-DPD method requires 271 multiplications while the MSA method requires 520 multiplications. Additionally, the condition number, time consumption and other similar statistics of OMSA-DPD methods also indicate that it is a better optimized.

The proposed OMSA performs efficiently, but its main advantage is

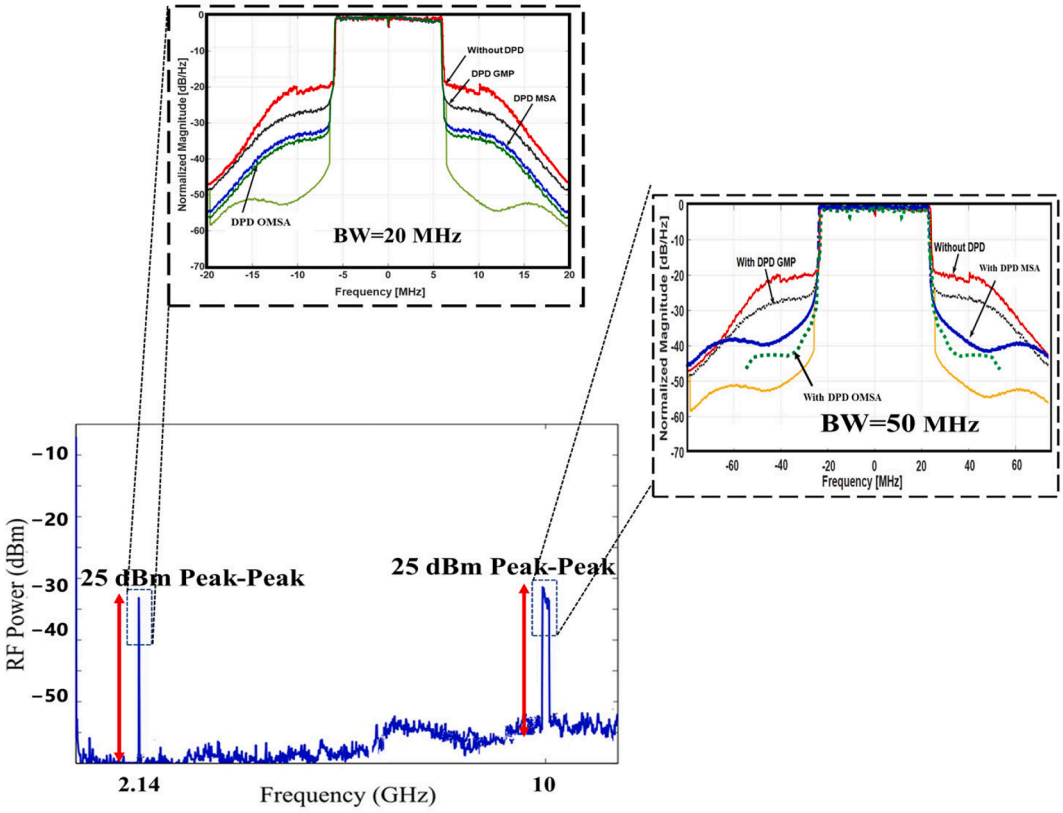

Fig. 5. Electrical Spectra received without DPD and with DPD GMP, MSA and OMSA.

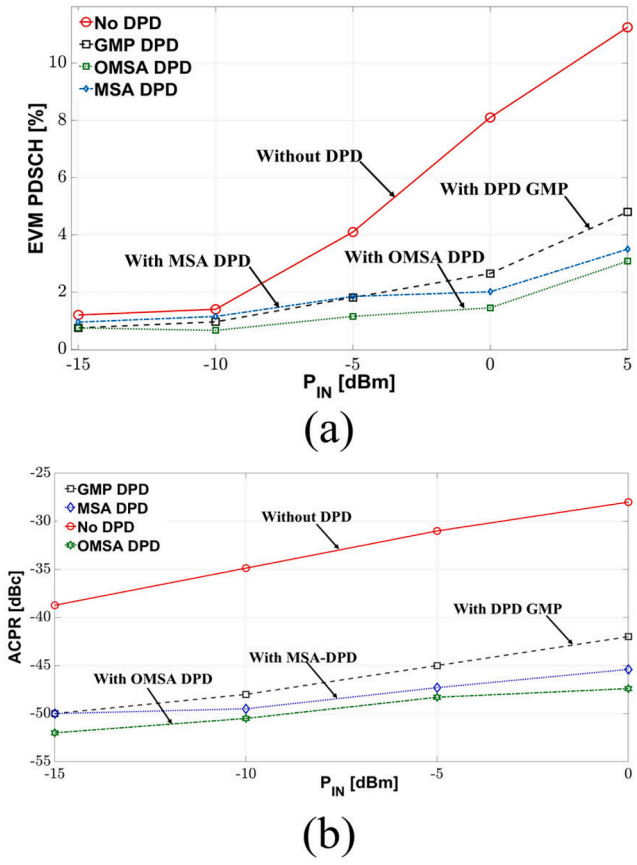

Fig. 6. DPD performance for changing RF input power with reference to: (a) EVM. (b) ACPR.

Table 2
Complexity Assessments.

Method	Coefficients	Multiplications
GMP	156	19,140
MSA	(K + 1) L*2(4 M + 1) = 520	(K + 1) (14 M + 2) = 220
OMSA	k (K + 1) *(4 M + 1)$x_{th}\|_{x_{th}=\beta}$ = 271	(14 M + 2)(K + 1)$x_{th}\|_{x_{th}=\beta}$ = 114

the significant reduction in complexity, which is particularly high in the case of ML DPD.

In addition to the comparison shown in Table 2, a comparison is drawn in terms of storage, memory and time consumption between OMSA, MSA and GMP methods which is shown in Fig. 7. The comparison clarifies that OMSA has much lesser complexity and achieves similar performance. This means that a balance between performance and complexity can be made in choosing the DPD complexity.

Table 3 summarizes the performance results at 0 dBm, where the OMSA-DPD technique demonstrates a reduction in complexity while maintaining similar performance compared to the MSA or GMP method.

6. Conclusion

The article presents a novel OMSA DPD method that enhances the previous MSA method for linearizing multiband 5G NR-based RoF link for eMBB applications. The proposed OMSA-based DPD method is a more optimized version of the MSA method, and it has been experimentally tested to transmit 5G NR waveforms at 2.14 GHz and 10 GHz over a 10 km fiber distance. The OMSA-DPD method is found to be slightly more efficient than the MSA method and it significantly reduces signal impairments, such as ACPR and EVM, in comparison to GMP methods, resulting in improved performance of the RoF link. Furthermore, the OMSA-DPD method requires significantly fewer multiplication operations, making it more efficient and less complex than the previous MSA method. To the best of the authors' knowledge, this is the first instance in which the performance of multiband 5G NR-based optical fronthaul has been improved and compared using a proposed OMSA DPD technique.

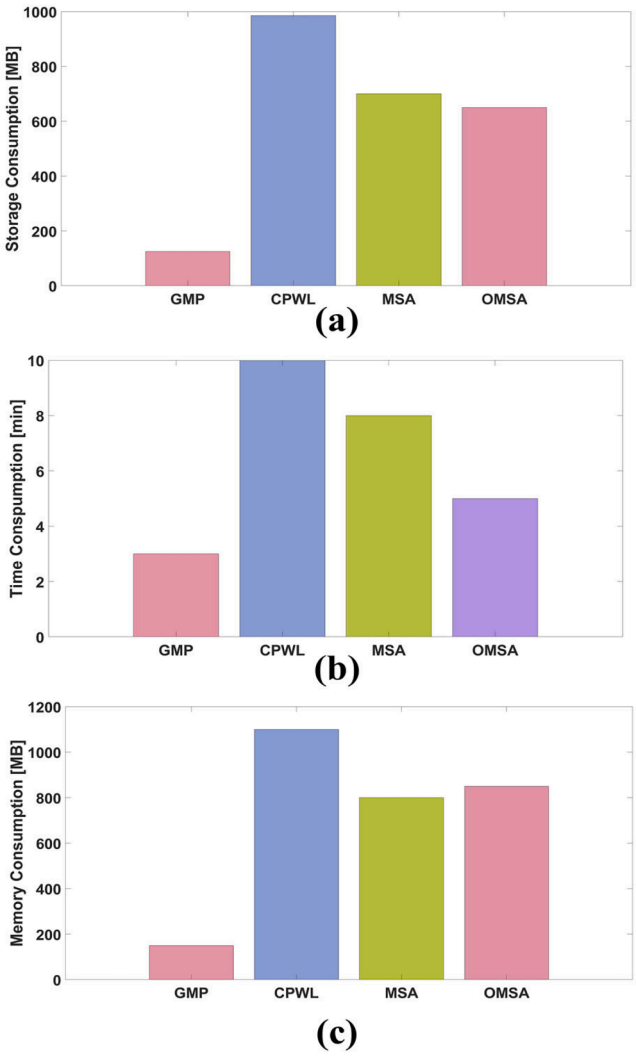

Fig. 7. Complexity Performance comparison for DPD architectures in terms of: (a) Storage Consumption (b) Memory Consumption (c) Time Consumption.

Table 3
Summary of the performance and complexity metrices.

Methodology	EVM (%)	ACLR (dBc)	Complexities		
			Coeffs	Time (min)	Memory (MB)
Without DPD	8	−27	–	–	–
GMP	4	−41	19,140	3	150
MSA	3	−44.4	220	8	800
OMSA	1.9	−46.1	114	5	850

CRediT authorship contribution statement

Muhammad Usman Hadi: Conceptualization, Data curation, Visualization, Investigation, Methodology, Software, Writing – original draft, Supervision, Validation, Writing – review & editing.

Declaration of Competing Interest

The authors declare that they have no known competing financial interests or personal relationships that could have appeared to influence the work reported in this paper.

Data availability

Data will be made available on request.

References

[1] ITU-R, IMT Vision–Framework and overall objectives of the future development of IMT for 2020 and beyond, 2015, Recommendation ITU-R M.2083-0, 1-19.
[2] J. Nanni, A. Giovannini, M.U. Hadi, E. Lenzi, S. Rusticelli, R. Wayth, F. Perini, J. Monari, G. Tartarini, Controlling Rayleigh-Backscattering-Induced Distortion in Radio Over Fibre Systems for Radioastronomic Applications, J. Light. Technol. 38 (2020) 5393–5405.
[3] A. Bogoni et al., "Modulation Index Study of a Cost-Effective Solution for CRAN Architecture Based on Coherent Radio-over-Fiber Backhaul," 2018 11th International Symposium on Communication Systems, (CSNDSP), 2018, pp. 1-4.
[4] J. Marti, J. Capmany, Microwave photonics and radio-over-fiber research, IEEE Microw. Mag. 10 (4) (June 2009) 96–105.
[5] L.u. Zhang, A. Udalcovs, R. Lin, O. Ozolins, X. Pang, L. Gan, R. Schatz, M. Tang, S. Fu, D. Liu, W. Tong, S. Popov, G. Jacobsen, W. Hu, S. Xiao, J. Chen, Toward Terabit Digital Radio over Fiber Systems: Architecture and Key Technologies, IEEE Commun. Mag. 57 (4) (2019) 131–137.
[6] H. Li, J. Bauwelinck, P. Demeester, G. Torfs, M. Verplaetse, J. Verbist, J. Van Kerrebrouck, L. Breyne, C.-Y. Wu, L. Bogaert, B. Moeneclaey, X. Yin, Real-Time 100-GS/s Sigma-Delta Modulator for All-Digital Radio-Over-Fiber Transmission, J. Lightwave Technol. 38 (2) (2020) 386–393.
[7] A. Hekkala, et al., Predistortion of Radio Over Fiber Links: Algorithms and Measurements, IEEE Trans. Circuits Syst. I Regul. Pap. 59 (3) (March 2012) 664–672.
[8] Y. Pei, X.u. Kun, J. Li, A. Zhang, Y. Dai, Y. Ji, J. Lin, Complexity-reduced digital predistortion for subcarrier multiplexed radio over fiber systems transmitting sparse multi-band RF signals, Opt. Express 21 (2013) 3708–3714.
[9] M.U. Hadi, P.A. Traverso, G. Tartarini, O. Venard, G. Baudoin, J.-L. Polleux, Digital Predistortion for Linearity Improvement of VCSEL-SSMF-Based Radio-Over-Fiber Links, IEEE Microw. Wireless Compon. Lett. 29 (2) (2019) 155–157.
[10] M.U. Hadi, C. Kantana, P.A. Traverso, G. Tartarini, O. Venard, G. Baudoin, J.-L. Polleux, Assessment of digital predistortion methods for DFB-SSMF radio-over-fiber links linearization, Microw Opt Technol Lett. 62 (2) (2020) 540–546.
[11] M.U. Hadi, M. Awais, M. Raza, K. Khurshid, H. Jung, Neural Network DPD for Aggrandizing SM-VCSEL-SSMF-Based Radio over Fiber Link Performance, Photonics 8 (2021) 19.
[12] J. He, J. Lee, S. Kandeepan, K. Wang, Machine Learning Techniques in Radio-over-Fiber Systems and Networks, Photonics 7 (2020) 105.
[13] M.U. Hadi, G. Murtaza, Enhancing distributed feedback-standard single mode fiber-radio over fiber links performance by neural network digital predistortion, Microw Opt Technol Lett. 63 (5) (2021) 1558–1565.
[14] Pereira, L. A. M., Lima, E. S., Mendes, L. L., & Cerqueira S. Jr., A.. (2023). Machine Learning-Based Digital Pre-Distortion Scheme for RoF Systems and Experimental 5G mm-waves Fiber-Wireless Implementation. *Journal of Microwaves, Optoelectronics and Electromagnetic Applications*, *22*(J. Microw. Optoelectron. Electromagn. Appl., 2023 22(1)), 172–183. https://doi.org/10.1590/2179-10742023v22i1270779.
[15] X. Xie, M. Hui, T. Liu, X. Zhang, Hybrid Linearization of Broadband Radio-Over-Fiber Transmission, IEEE Photon. Technol. Lett. 30 (8) (2018) 692–695, https://doi.org/10.1109/LPT.2018.2812745.
[16] J. Nanni et al., "Effective Digital Pre-Distortion Loop for Front Hauls based on short-λ-VCSELs over pre-existent G-652 Infrastructures," 2021 International Topical Meeting on Microwave Photonics (MWP), Pisa, Italy, 2021, pp. 1-4, doi: 10.1109/MWP53341.2021.9639378.
[17] I.A. Rather, G. Kumar, R. Saha, Survey on RoF technology and the mitigation schemes over the challenges in the RoF network, Optik 247 (2021), 168007.
[18] M.U. Hadi, N. Soin, S. Kausar, Enhancing 5G multi-band long haul optical fronthaul links performance by magnitude-selective affine digital predistortion method, Microw Opt Technol Lett. (2022) 827–834.
[19] G. Kalfas, N. Pleros, An Agile and Medium-Transparent MAC Protocol for 60 GHz Radio-Over-Fiber Local Access Networks, J. Lightwave Technol. 28 (16) (2010) 2315–2326.
[20] 3GPP TS 8.141–1 and 8.141–2 v1.1.0, 3rd Generation Partnership Project; Base Station (BS) conformance testing.
[21] 3GPP TR 21.916 V16.2.0 (2022-06) Release 16.
[22] 3GPP TS 6.141 version 17.5.0 Release 17.